Uncovering Quantum Correlations with Time-Multiplexed Click Detection

J. Sperling, M. Bohmann, and W. Vogel
Arbeitsgruppe Theoretische Quantenoptik, Institut für Physik, Universität Rostock, D-18051 Rostock, Germany

G. Harder, B. Brecht, V. Ansari, and C. Silberhorn
Integrated Quantum Optics Group, Applied Physics, University of Paderborn, 33098 Paderborn, Germany
(Received 27 March 2015; published 7 July 2015)

We report on the implementation of a time-multiplexed click detection scheme to probe quantum correlations between different spatial optical modes. We demonstrate that such measurement setups can uncover nonclassical correlations in multimode light fields even if the single mode reductions are purely classical. The nonclassical character of correlated photon pairs, generated by a parametric down-conversion, is immediately measurable employing the theory of click counting instead of low-intensity approximations with photoelectric detection models. The analysis is based on second- and higher-order moments, which are directly retrieved from the measured click statistics, for relatively high mean photon numbers. No data postprocessing is required to demonstrate the effects of interest with high significance, despite low efficiencies and experimental imperfections. Our approach shows that such novel detection schemes are a reliable and robust way to characterize quantum-correlated light fields for practical applications in quantum communications.

DOI: 10.1103/PhysRevLett.115.023601 PACS numbers: 42.50.Ar, 03.65.Wj, 42.50.Dv, 42.50.Xa

Introduction.—Certifying quantum features of light is one key requirement for optical implementations of quantum-information technology [1,2]. This requires, on the one hand, reliable sources for correlated quantum light and, on the other hand, appropriate detection schemes [3,4]. Since correlations between different degrees of freedom can have different origins in quantum optics, they might be covered by classical statistical optics, or they are genuine quantum properties having no such classical counterpart. Using the classical theory of coherence, one way to discern quantum from classical effects has been introduced independently by Glauber [5] and Sudarshan [6].

A quantum-state characterization is often based on the photon number distribution, see, e.g., Refs. [7,8]. The corresponding photoelectric detection theory yields Poissonian statistics for coherent light. However, detectors that directly measure photon numbers are typically not available or require advanced data postprocessing [9,10]. Today, quantum states with low mean photon number are often detected with avalanche photodiodes (APDs) in the Geiger mode, which basically produce a “click” if any number of photons is absorbed, and remain silent otherwise. A uniform splitting of a radiation field with many photons into portions of lower intensities, each being measured with an APD, can extent the knowledge about the signal, for example, to discriminate single- and two-photon events. Various kinds of such photon-number-resolving detectors have been implemented to demonstrate nonclassical features of radiation fields, e.g., in Refs. [11–17], or for characterizing the non-Poissonian behavior of the click statistics [18,19]. One particular realization of such a scheme that requires only a small number of optical elements is so-called time-bin multiplexing detectors (TMDs) [18,20,21], cf. Fig. 1. Based on these TMDs, one can reconstruct nonclassical features of quantum light fields [22,23] or higher-order correlation functions [24].

The proper theoretical detection model for such devices is a quantum version of the binomial statistics [25]. It was also shown that approximating these statistics with a Poissonian distribution and applying quantumness probes of the photon statistics can yield fake signatures of nonclassicality for classical fields—even if the number

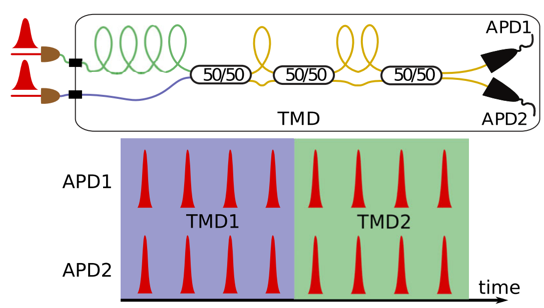

FIG. 1 (color online). The realization of two TMDs in a single device is depicted. One part (upper, green input) of the correlated signal field is delayed in an optical fiber before entering the device. Within the TMD, any signal is split by a 50:50 beam splitter followed by another delay line in one output. This multiplexing is done three times yielding 2^3 separated time bins for each (upper green and lower blue) input field, which are measured with two APDs.

of registered signal photons is 1 order of magnitude below the number of time bins. To eliminate these errors, nonclassicality criteria in terms of moments of the click-counting statistics have been proposed to directly uncover quantum light with click counters without data postprocessing [26]. For example, the notion of sub-binomial light has been introduced [27] and experimentally demonstrated [28,29].

In the present work, we report on the characterization of a bipartite quantum-correlated light source using click detectors only. We demonstrate that click detection is capable of directly verifying nonclassicality even for imperfect experimental settings. For our parametric down-conversion (PDC) based light source, this approach correctly shows classical single-mode correlations and, at the same time, it uncovers quantum correlations between the modes. We show that our simple treatment to infer these quantum features works for a broad range of pump powers. In particular, it works increasingly well for increasing pump powers, where the often used weak signal approximations with the photoelectric detection theory completely break down, as we will show later.

Nonclassical moments of the click statistics.—The probability to measure k_A clicks within the $N = 8$ time bins assigned to the signal A together with k_B clicks from the signal B, cf. Fig. 1, is described through the joint click-counting statistics [25,26]:

$$c_{k_A,k_B} = \left\langle : \binom{N}{k_A} \hat{m}_A^{N-k_A} (\hat{1}_A - \hat{m}_A)^{k_A} \times \binom{N}{k_B} \hat{m}_B^{N-k_B} (\hat{1}_B - \hat{m}_B)^{k_B} : \right\rangle, \quad (1)$$

with $:\cdots:$ denoting the normally ordering prescription and $\hat{m}_i = e^{-\Gamma(\hat{n}_i/N)}$ for the modes $i = A, B$. In general, Γ can be an unknown detector response, being a function of the photon number operators $\hat{n}_i$. For example, a linear form of the response function is $\Gamma(\hat{n}_i/N) = \eta\hat{n}_i/N + \nu$, with η and ν being the quantum efficiency and the dark count rate, respectively.

In Ref. [26] it has been demonstrated that the matrix of click moments $M^{(K_A,K_B)}$ is non-negative for any classical light field,

$$0 \leq M^{(K_A,K_B)} = (\langle : \hat{m}_A^{s_A+t_A} \hat{m}_B^{s_B+t_B} : \rangle)_{(s_A,s_B),(t_A,t_B)} \quad (2)$$

with $s_i, t_i = 0, \ldots, K_i/2 \leq N/2$ for even K_i and N. The superscript (K_A, K_B) defines the highest moment of each subsystem within the matrix M; see also Ref. [30]. For instance, the single-mode and bipartite, second-order matrices of click moments are

$$M^{(2,0)} = \begin{pmatrix} 1 & \langle : \hat{m}_A : \rangle \\ \langle : \hat{m}_A : \rangle & \langle : \hat{m}_A^2 : \rangle \end{pmatrix},$$

$$M^{(0,2)} = \begin{pmatrix} 1 & \langle : \hat{m}_B : \rangle \\ \langle : \hat{m}_B : \rangle & \langle : \hat{m}_B^2 : \rangle \end{pmatrix}, \quad \text{and}$$

$$M^{(2,2)} = \begin{pmatrix} 1 & \langle : \hat{m}_A : \rangle & \langle : \hat{m}_B : \rangle \\ \langle : \hat{m}_A : \rangle & \langle : \hat{m}_A^2 : \rangle & \langle : \hat{m}_A \hat{m}_B : \rangle \\ \langle : \hat{m}_B : \rangle & \langle : \hat{m}_A \hat{m}_B : \rangle & \langle : \hat{m}_B^2 : \rangle \end{pmatrix}, \quad (3)$$

respectively. The needed moments can be directly retrieved from the measured click-counting statistics [26]

$$\langle : \hat{m}_A^{l_A} \hat{m}_B^{l_B} : \rangle = \sum_{k_A=0}^{N-l_A} \sum_{k_B=0}^{N-l_B} \frac{\binom{N-k_A}{l_A}\binom{N-k_B}{l_B}}{\binom{N}{l_A}\binom{N}{l_B}} c_{k_A,k_B}. \quad (4)$$

One way to probe the character of nonclassical correlations, i.e., violating inequality (2), can be done as follows. We have nonclassical Kth-order click correlations if

$$M^{(K,0)} \geq 0, M^{(0,K)} \geq 0, \quad \text{and} \quad M^{(K,K)} \ngeq 0. \quad (5)$$

This means that both Kth-order single-mode marginals are classical and the bimodal, Kth-order correlation matrix is nonclassical, i.e., it has at least one negative eigenvalue. In order to genuinely certify such nonclassical correlations, it is sufficient to consider the minimal eigenvalues of the click-moment matrices. Say $\vec{f}_A$, $\vec{f}_B$, and $\vec{f}_{AB}$ are the normalized eigenvectors to the minimal eigenvalues e_A, e_B, and e_{AB} of $M^{(K,0)}$, $M^{(0,K)}$, and $M^{(K,K)}$, respectively. Now, definition (5) is rewritten as

$$e_A = \vec{f}_A^{\dagger} M^{(K,0)} \vec{f}_A \geq 0,$$

$$e_B = \vec{f}_B^{\dagger} M^{(0,K)} \vec{f}_B \geq 0, \quad \text{and}$$

$$e_{AB} = \vec{f}_{AB}^{\dagger} M^{(K,K)} \vec{f}_{AB} < 0. \quad (6)$$

This method will serve as our approach to determine Kth-order quantum correlations between the subsystems A and B, see Ref. [30] for further details.

Implementation and model.—The states under study are produced in a type II PDC in a periodically poled, 8 mm long KTP waveguide. The PDC process is pumped with 1ps long pulses at a repetition rate of 70 kHz and a wavelength of 768 nm coming from a Ti:sapphire laser. The states are generated in two orthogonally polarized signal and idler modes at 1536 nm. In the regime of less than one photon per pulse, the source has been characterized in Ref. [31] with emphasis on the modal properties, and genuine single-mode operation of the PDC has been shown. Behind the waveguide, broadband spectral filters are used to suppress the pump and unwanted background outside of the PDC spectral region. Signal and idler modes are then split at a polarizing beam splitter and coupled into a two-mode TMD consisting of a fiber network with 50:50 beam splitters and a pair of InGaAs APDs as depicted in Fig. 1. For each pump setting, we record the full time tagging data for 10 min and translate them into the click statistics of all possible 8×8 click events. Experimental imperfections are unbalanced beam splitters within our TMD, i.e., splitting ratios that slightly deviate from 50:50, or after-pulsing effects [32]. We minimized both effects through a careful setup preparation.

The PDC may be formulated in terms of the effective Hamiltonian $\hat{H} = i\kappa\gamma\hat{a}^\dagger\hat{b}^\dagger + \text{H.c.}$, where κ is a coupling constant, γ is the coherent amplitude of the pump beam, and $\hat{a}^\dagger$ $(\hat{b}^\dagger)$ is the creation operator of the mode $A\,(B)$. An idealized, perfect unitary evolution for this process yields the two-mode squeezed-vacuum state

$$|\xi\rangle = e^{\xi(\hat{a}^\dagger\hat{b}^\dagger - \hat{a}\,\hat{b})}|\text{vac}\rangle = \sum_{n=0}^{\infty}\frac{(\tanh\xi)^n}{\cosh\xi}|n\rangle_A|n\rangle_B, \qquad (7)$$

where $\xi \geq 0$ is proportional to the square root of the pump power P, since $\hat{H} \propto \gamma$ and $P \propto \gamma^2$. The noise suppression of the squeezed quadrature $\hat{X}$ is $\langle[\Delta\hat{X}]^2\rangle = e^{-2\xi}\langle[\Delta\hat{X}]^2\rangle_{\text{vac}}$ [7,30]. Because of the pairwise generation of photons, the state (7) has perfect photon-number correlations. This means that whenever a certain number of photons is present in one mode, the same number of photons occurs in the other mode. However, the click-counting statistics include off-diagonal elements $c_{k_A,k_B} \neq 0$ for $k_A \neq k_B$, even for a perfect detection without dark counts and unit efficiency, cf. Fig. 2. This difference between click-counting and photoelectric detection is due to a finite probability that more than one photon can end in the same time bin. It is worth mentioning that the single-mode reduced states $\text{tr}_A|\xi\rangle\langle\xi|$ and $\text{tr}_B|\xi\rangle\langle\xi|$ are classical thermal states, and that the total number of photons is $\bar{n} = \langle\xi|\hat{n}_A + \hat{n}_B|\xi\rangle = 2\sinh^2\xi$.

Second-order correlations.—First, let us focus on second-order click correlations, cf. Eq. (3), which include the information about the mean values, the variances, and the covariance of the joint click-counting statistics [26]. In Fig. 3, we plot the measurement results. Using the approach in Eq. (6), the minimal eigenvalues e_{AB} (top), e_A (Fig. 3, bottom, left), and e_B (Fig. 3, bottom, right) are shown in their dependence on the energy per pulse, $E_{\text{pump}} = P/70$ kHz. The energy can be experimentally controlled. The single-mode matrices are non-negative, $e_A \geq 0$ and $e_B \geq 0$, whereas the cross correlations are nonclassical, $e_{AB} < 0$. Thus, we have verified the quantum nature of the second-order click correlations between the spatial modes A and B.

In order to compare our measured results, a simple theoretical model is used. We assume that the pure state (7) is generated, and the detectors are described via a plain linear response function: $\Gamma(\hat{n}/N) = \eta\hat{n}/N + \nu$. As we discussed above, the parameter ξ, characterizing the state $|\xi\rangle$, depends on the pump power P: $\xi = \xi_0\sqrt{P}$. The proportionality constant ξ_0, the quantum efficiency η, and the dark count rate have been fitted using the standard method of least squares. They are $\eta = 9.6\%$, $\nu = 0.51$, and $\xi_0 = 0.087\ (\mu\text{W})^{-1/2}$. With these values, we estimate the total mean photon numbers to be 0.9–15 photons for the pump powers 50–403μW or energies 0.7–5.8 nJ. Already

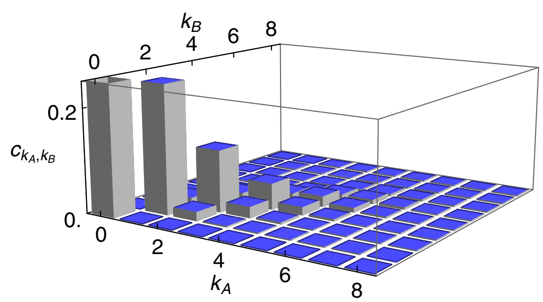

FIG. 2 (color online). The joint click-counting statistics (1) for the state (7), $\xi = 1$, and a perfect linear response $\Gamma(\hat{n}/N) = \hat{n}/N$. The probability for no clicks is cut, $c_{0,0} = 0.42$. Even though we have perfect photon correlations, the click-counting distribution includes off-diagonal terms.

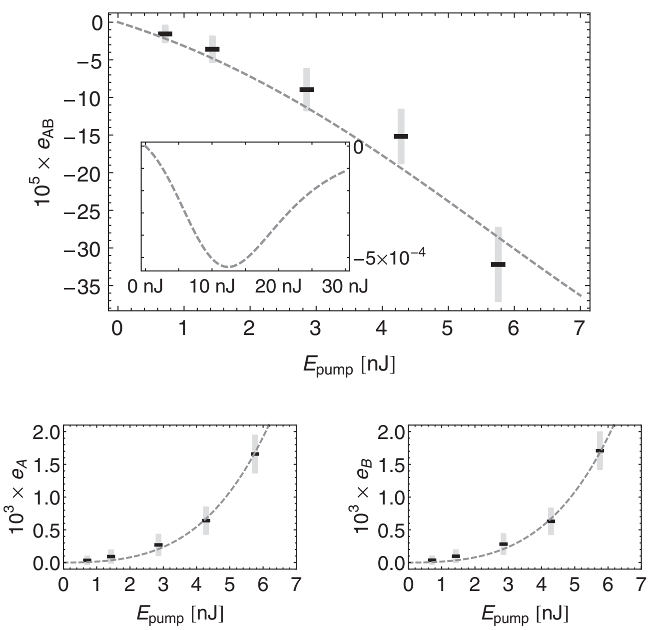

FIG. 3. The upper plot shows the minimal eigenvalue e_{AB} (black bars) of the experimentally obtained matrix of moments $M^{(2,2)}$ depending on the pump energy E_{pump}. Error bars are given as gray areas. The dashed curve is the theoretical prediction. The inset depicts the continuation of the theoretical curve for higher energies including saturation effects. The lower plots show the minimal eigenvalues e_A and e_B of $M^{(2,0)}$ (left) and $M^{(0,2)}$ (right), respectively, a 10 standard deviations error bar, and the theoretical prediction. Since the bimodal correlations are negative and the single-mode reductions are non-negative, we successfully determined nonclassical correlations between the modes A and B.

this simplified model yields a good agreement with the measured results, which highlights the excellent performance of the engineered PDC source, cf. the dashed lines in Fig. 3.

The inset in the upper plot shows the extrapolation of the quantum correlations, $e_{AB} < 0$, for higher pump energies. At some point, the mean photon number is so high that these correlations saturate and eventually vanish. A high squeezing level and a classical laser light with a large coherent amplitude result in the same signal—all time bins are occupied with a large number of photons. Therefore, at high photon numbers, the signals of nonclassical and classical states cannot be discriminated. Thus, the recorded quantum correlations of the former state must decrease due to the saturation of click-counting devices, which is automatically included in the click-counting theory. Imperfections are also studied [30].

Let us emphasize again that the states have been generated for pump powers ranging over almost 1 order of magnitude. Verifying nonclassical photon-photon correlations in this comparably large domain is typically considered a challenging task, but can easily be accomplished with our TMD click counters. In addition, since the method of nonclassical click moments is independent of the state, the verified quantum correlations can be certified even if the pump power was completely unknown.

Higher-order correlations.—Let us study higher-order quantum correlations. They become particularly meaningful when second-order criteria fail to properly characterize the state [33]. For example, the third- and fourth-order moment relate to the so-called skewness and the flatness (or kurtosis), respectively. The highest possible order of moments one can infer from $N = 8$ time bins per mode is $K = 8$ in Eqs. (2) and (6), which yields a full characterization of the click-counting statistics.

The bound for a classical signal $M^{(K,K)} \geq 0$ is given by the eigenvalue $e_{\mathrm{cl}} = 0$ [26]. Thus, the signed distance, in units of standard deviations, of the experimentally obtained minimal eigenvalue $e = \bar{e} \pm \Delta e$ to this classical bound leads to a signed significance

$$\Sigma = \frac{\bar{e} - e_{\mathrm{cl}}}{\Delta e} = \frac{\bar{e}}{\Delta e}, \tag{8}$$

representing a signed relative error. A negative significance $\Sigma < 0$ verifies the nonclassicality with a significance of $|\Sigma|$. Typically, $\Sigma \lesssim -3$ is a significant verification of the negativity, whereas $\Sigma \approx 0$ cannot be distinguished from the classical bound 0.

In Fig. 4, the significance levels of the full eighth-order quantum correlation within $M^{(8,8)}$ are given. The single-mode, signed significances for $M^{(8,0)}$ and $M^{(0,8)}$ can be found in Ref. [30]. There are no significant eighth-order, single-mode correlations $M^{(8,0)}, M^{(0,8)} \gtrsim 0$—the largest single-mode negativities are of the order of $\Sigma \sim -10^{-5}$.

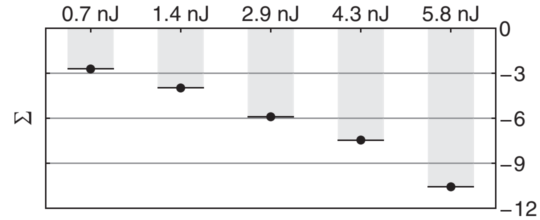

FIG. 4. The signed significances Σ of the largest negativities of the full matrix of click moments $M^{(8,8)}$ are shown. The highest significance levels of nonclassicality between the subsystems are verified for our highest energy. In this region the impact of the click-counting theory is most pronounced.

Additionally, the significance of negativities in $M^{(8,8)}$, cf. Fig. 4, are in the range of 2.7–10.6 for the energies 0.7–5.8 nJ, respectively. Hence, for most of the energies, a significant eighth-order nonclassical correlation between the modes A and B is certified. Remarkably, the significance even increases with the energy, which is due to an improved signal-to-noise ratio with increasing mean photon numbers, because the no-click event has a much lower probability in this regime.

On the one hand, one would typically not use such comparably high intensities in our measurement setup, when analyzing the data with the inappropriate photoelectric detection model. In this case, the single-mode signed significances evaluate to −2.4 to −13, cf. Ref. [30], suggesting fake nonclassicality, which worsens with increasing pump power. On the other hand, our consistent treatment in terms of the click statistics correctly identifies higher-order bimodal correlations while showing, as expected for our source, no nonclassicality in the single-mode marginals.

Here, we studied photon-photon correlations in terms of click-counting moments for high mean photon numbers. Even though we have an incomplete knowledge about the state—no phase information and only a finite number of bins—we are able to uncover quantum correlations. The lack of phase resolution compares to a fully phase randomized version of the state (7), which has been shown to include nonclassical correlations without entanglement [34], being certified with the present method. The measurement scheme may be complemented for phase-sensitive measurements [35], to infer squeezing or entanglement.

Conclusions.—We set up a click correlation measurement scheme using time-multiplexed detectors for probing nonclassical correlations of a bipartite quantum light field. We could directly infer nonclassical correlations from the measured joint click-counting statistics with high significances. This was possible despite a low detection efficiency, estimated as 10%, and over 1 order of magnitude of intensities. Note that the bare click data have been analyzed without corrections for imperfections or related postprocessing techniques. We compared our results with a theoretical model and obtained a very good agreement.

In particular, the expectation of this model—all orders of single-mode correlations do not exhibit nonclassicality, but the two-mode correlations do—is correctly demonstrated with our method. This underlines the functionality of our device for verifying genuine quantum correlations between spatial optical modes.

Our proposed measurement together with the click-detection analysis is a robust and efficient tool to characterize quantum light. We believe that this simplicity of click detection—being solely a collection of probabilities of coincidence clicks—paves the way towards real-live implementations of quantum communication protocols in optical systems. The present approach may be further generalized to handle more complex types of quantum-correlated, multimode radiation fields.

J. S., M. B., and W. V. acknowledge financial support by Deutsche Forschungsgemeinschaft through SFB 652 and VO 501/22-1. G. H., B. B., V. A., and C. S. acknowledge funding from the European Community's Seventh Framework Program FP7/2001-2013 under Grant Agreement No. 248095 through the Integrated Project Q-ESSENCE.

Note added.—We recently became aware of a related paper in preparation by the group of I. A. Walmsley and co-workers [36].

[1] P. Kok, W. J. Munro, K. Nemoto, T. C. Ralph, J. P. Dowling, and G. J. Milburn, Linear optical quantum computing with photonic qubits, Rev. Mod. Phys. **79**, 135 (2007).
[2] A. Datta, L. Zhang, N. Thomas-Peter, U. Dorner, B. J. Smith, and I. A. Walmsley, Quantum metrology with imperfect states and detectors, Phys. Rev. A **83**, 063836 (2011).
[3] G. S. Buller and R. J. Collins, Single-photon generation and detection, Meas. Sci. Technol. **21**, 012002 (2010).
[4] M. D. Eisaman, J. Fan, A. Migdall, and S. V. Polyakov, Single-photon sources and detectors, Rev. Sci. Instrum. **82**, 071101 (2011).
[5] R. J. Glauber, Photon Correlations, Phys. Rev. Lett. **10**, 84 (1963); Coherent and incoherent states of the radiation field, Phys. Rev. **131**, 2766 (1963).
[6] E. C. G. Sudarshan, Equivalence of Semiclassical and Quantum Mechanical Descriptions of Statistical Light Beams, Phys. Rev. Lett. **10**, 277 (1963).
[7] G. S. Agarwal, *Quantum Optics* (Cambridge University Press, Cambridge, 2013).
[8] L. Mandel and E. Wolf, *Optical Coherence and Quantum Optics* (Cambridge University Press, Cambridge, 1995).
[9] O. Haderka, J. Peřina, Jr., M. Hamar, and J. Peřina, Direct measurement and reconstruction of nonclassical features of twin beams generated in spontaneous parametric down-conversion, Phys. Rev. A **71**, 033815 (2005).
[10] V. N. Starkov, A. A. Semenov, and H. V. Gomonay, Numerical reconstruction of photon-number statistics from photocounting statistics: Regularization of an ill-posed problem, Phys. Rev. A **80**, 013813 (2009).
[11] E. Waks, E. Diamanti, B. C. Sanders, S. D. Bartlett, and Y. Yamamoto, Direct Observation of Nonclassical Photon Statistics in Parametric Down-Conversion, Phys. Rev. Lett. **92**, 113602 (2004).
[12] A. Allevi, M. Bondani, and A. Andreoni, Photon-number correlations by photon-number resolving detectors, Opt. Lett. **35**, 1707 (2010).
[13] G. Puentes, A. Datta, A. Feito, J. Eisert, M. B. Plenio, and I. A. Walmsley, Entanglement quantification from incomplete measurements: applications using photon-number-resolving weak homodyne detectors, New J. Phys. **12**, 033042 (2010).
[14] J. F. Dynes, Z. L. Yuan, A. W. Sharpe, O. Thomas, and A. J. Shields, Probing higher order correlations of the photon field with photon number resolving avalanche photodiodes, Opt. Express **19**, 13268 (2011).
[15] P.-A. Moreau, J. Mougin-Sisini, F. Devaux, and E. Lantz, Realization of the purely spatial Einstein-Podolsky-Rosen paradox in full-field images of spontaneous parametric down-conversion, Phys. Rev. A **86**, 010101(R) (2012).
[16] L. Dovrat, M. Bakstein, D. Istrati, E. Megidish, A. Halevy, L. Cohen, and H. S. Eisenberg, Direct observation of the degree of correlations using photon-number-resolving detectors, Phys. Rev. A **87**, 053813 (2013).
[17] G. Donati, T. J. Bartley, X.-M. Jin, M.-D. Vidrighin, A. Datta, M. Barbieri, and I. A. Walmsley, Observing optical coherence across Fock layers with weak-field homodyne detectors, Nat. Commun. **5**, 5584 (2014).
[18] M. J. Fitch, B. C. Jacobs, T. B. Pittman, and J. D. Franson, Photon-number resolution using time-multiplexed single-photon detectors, Phys. Rev. A **68**, 043814 (2003).
[19] J.-L. Blanchet, F. Devaux, L. Furfaro, and E. Lantz, Measurement of Sub-Shot-Noise Correlations of Spatial Fluctuations in the Photon-Counting Regime, Phys. Rev. Lett. **101**, 233604 (2008).
[20] J. Řeháček, Z. Hradil, O. Haderka, J. Peřina Jr., and M. Hamar, Multiple-photon resolving fiber-loop detector, Phys. Rev. A **67**, 061801(R) (2003).
[21] D. Achilles, C. Silberhorn, C. Śliwa, K. Banaszek, and I. A. Walmsley, Fiber-assisted detection with photon number resolution, Opt. Lett. **28**, 2387 (2003).
[22] K. Laiho, K. N. Cassemiro, D. Gross, and C. Silberhorn, Probing the Negative Wigner Function of a Pulsed Single Photon Point by Point, Phys. Rev. Lett. **105**, 253603 (2010).
[23] G. Harder, C. Silberhorn, J. Rehacek, Z. Hradil, L. Motka, B. Stoklasa, and L. L. Sánchez-Soto, Time-multiplexed measurements of nonclassical light at telecom wavelengths, Phys. Rev. A **90**, 042105 (2014).
[24] M. Avenhaus, K. Laiho, M. V. Chekhova, and C. Silberhorn, Accessing Higher Order Correlations in Quantum Optical States by Time Multiplexing, Phys. Rev. Lett. **104**, 063602 (2010).
[25] J. Sperling, W. Vogel, and G. S. Agarwal, True photocounting statistics of multiple on-off detectors, Phys. Rev. A **85**, 023820 (2012).
[26] J. Sperling, W. Vogel, and G. S. Agarwal, Correlation measurements with on-off detectors, Phys. Rev. A **88**, 043821 (2013).
[27] J. Sperling, W. Vogel, and G. S. Agarwal, Sub-binomial Light, Phys. Rev. Lett. **109**, 093601 (2012).

[28] T. J. Bartley, G. Donati, X.-M. Jin, A. Datta, M. Barbieri, and I. A. Walmsley, Direct Observation of Sub-binomial Light, Phys. Rev. Lett. **110**, 173602 (2013).

[29] R. Heilmann, J. Sperling, A. Perez-Leija, M. Gräfe, M. Heinrich, S. Nolte, W. Vogel, and A. Szameit, Divide-and-conquer: An integrated photon-counting scheme, arXiv:1502.04932.

[30] See Supplemental Material at http://link.aps.org/supplemental/10.1103/PhysRevLett.115.023601 for the data processing with our approach and all results of the analysis.

[31] G. Harder, V. Ansari, B. Brecht, T. Dirmeier, C. Marquardt, and C. Silberhorn, An optimized photon pair source for quantum circuits, Opt. Express **21**, 13975 (2013).

[32] Y. Kang, H. X. Lu, and Y.-H. Lo, Dark count probability and quantum efficiency of avalanche photodiodes for single-photon detection, Appl. Phys. Lett. **83**, 2955 (2003).

[33] G. S. Agarwal and K. Tara, Nonclassical character of states exhibiting no squeezing or sub-Poissonian statistics, Phys. Rev. A **46**, 485 (1992).

[34] A. Ferraro and M. G. A. Paris, Nonclassicality Criteria from Phase-Space Representations and Information-Theoretical Constraints are Maximally Inequivalent, Phys. Rev. Lett. **108**, 260403 (2012); E. Agudelo, J. Sperling, and W. Vogel, Quasiprobabilities for multipartite quantum correlations of light, Phys. Rev. A **87**, 033811 (2013).

[35] J. Sperling, W. Vogel, and G. S. Agarwal, Balanced homodyne detection with on-off detector systems: Observable nonclassicality criteria, Europhys. Lett. **109**, 34001 (2015); A. Luis, J. Sperling, and W. VogelNonclassicality Phase-Space Functions: More Insight with Fewer Detectors, Phys. Rev. Lett. **114**, 103602 (2015).

[36] T. J. Bartley *et al.* (unpublished)